

THE EFFECTS OF SHOCK WAVE COMPACTION ON THE TRANSITION

TEMPERATURES OF A15 STRUCTURE SUPERCONDUCTORS
(NASA-CR-120708) THE EFFECTS OF SHOCK WAVE
COMPACTION ON THE TRANSITION TEMPERATURES OF
A15 STRUCTURE SUPERCONDUCTORS Final Report
(Alabama Univ., Huntsville.) 51 p HC \$4.25

N75-20126

Unclas

CSCL 20L G3/76 14458

by

Guenther H. Otto

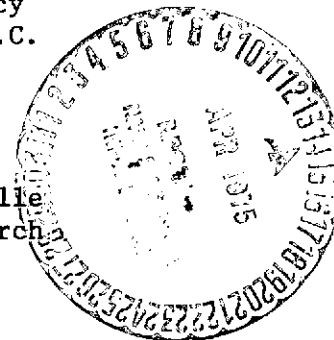
Final Report

This research work was supported by
the National Aeronautics and Space Administration
George C. Marshall Space Flight Center
Contract NAS8-30244

and by

the Advanced Research Projects Agency
Department of Defense, Washington, D.C.

The University of Alabama in Huntsville
School of Graduate Studies and Research
P. O. Box 1247
Huntsville, Alabama 35807



August 1974

THE EFFECTS OF SHOCK WAVE COMPACTION ON THE TRANSITION
TEMPERATURES OF A15 STRUCTURE SUPERCONDUCTORS

by

Guenther H. Otto

Final Report

This research work was supported by
the National Aeronautics and Space Administration
George C. Marshall Space Flight Center
Contract NAS8-30244

and by

the Advanced Research Projects Agency
Department of Defense, Washington, D.C.

The University of Alabama in Huntsville
School of Graduate Studies and Research
P. O. Box 1247
Huntsville, Alabama 35807

August 1974

TABLE OF CONTENTS

	<u>Page</u>
ACKNOWLEDGEMENTS	i
ILLUSTRATIONS	ii
TABLES	iii
PREFACE	iv
ABSTRACT	v
I. INTRODUCTION	1
II. SAMPLE PREPARATION AND CHARACTERIZATION	3
1. Cast Specimens	3
2. Pulverization	6
3. Shock Wave Generation	7
4. Low Temperature Set-up	10
5. Optical, X-ray, and Microprobe Analysis	13
III. EXPERIMENTAL RESULTS	14
1. Appearance of Compacted Compound Powders	14
2. Superconductivity of Compacted Compound Powders	16
3. Microstructure of Compacted V_3Si	26
4. Shock Wave Compaction of Pure Niobium Powder	29
5. Attempted Synthesis of Nb_3Ge from its Constituents	32
IV. SHOCK WAVE PROPAGATION	37
V. CONCLUSIONS AND RECOMMENDATIONS	41
REFERENCES	

ACKNOWLEDGEMENTS

We would like to thank the Explosives Management Team (Leader Mr. C. Saxon) of the Redstone Arsenal, Alabama, for their understanding cooperation in the sample preparation. The X-ray microprobe analyses of the Nb-Ge specimens were kindly supplied by Mr. G. Horn and the DODUCO K. G., Pforzheim/West Germany. Mr. D. Gates of MSFC-Space Sciences Laboratory performed the scanning electron micrographic investigations. The support of Mr. D. Homesley and Mr. O. Y. Reece in evaluating the results is greatly appreciated. We would like also to express our thanks to Dr. C. C. Koch and Mr. J. Scarbrough of the Oak Ridge National Laboratory for the provision of the arc furnace and their valuable assistance in the preparation of the cast specimens. The necessary cryogenic equipment was provided by MSFC-Space Sciences Laboratory and we thank Dr. E. W. Urban and Dr. L. L. Lacy for their stimulating interest in this project.

ILLUSTRATIONS

- Figure 1. Transition curves of Nb_3Al and $\text{Nb}_3(\text{Al},\text{Ge})$ cast samples.
- Figure 2. Schematic representation of the converging shock wave technique for powder compaction.
- Figure 3. Block diagram for inductive measurement of T_c .
- Figure 4. Block diagram for resistive measurement of T_c .
- Figure 5. Photomicrographs of shock wave compacted compound powders.
- Figure 6. Photomicrographs of shock wave compacted compound powders.
- Figure 7. Superconducting transition curves for $\text{Nb}_3(\text{Al},\text{Ge})$ in bulk, pulverized, and shock compacted state.
- Figure 8. Superconducting transition curves for $\text{Nb}_3(\text{Al},\text{Ge},\text{Si})$ in bulk, pulverized, and shock compacted state.
- Figure 9. Superconducting transition curves for Nb_3Al in bulk, pulverized, and shock compacted state.
- Figure 10. Superconducting transition curves for V_3Si in bulk, pulverized, and shock compacted state.
- Figure 11. Superconducting transition curves for V_3Si in bulk and shock compacted state.
- Figure 12. Scanning electron micrographs of V_3Si powder before and after shock wave compaction.
- Figure 13. Scanning electron micrographs of V_3Si powder after shock wave compaction.
- Figure 14. Shock compacted niobium powder with central remelt area.
- Figure 15. Scanning electron micrograph of compacted 3Nb:1Ge powder mixture.
- Figure 16. X-ray microprobe analysis of a compacted 3Nb:1Ge powder mixture.
- Figure 17. Relationship of detonation velocity and charge density for nitroguanidine.

TABLES

- TABLE 1. Selected Data for Cast Compound Specimens.
- TABLE 2. Data for Shock Wave Compacted Compound Powders.
- TABLE 3. Properties of Shock Compacted Niobium Powder.
- TABLE 4. Characteristic Data for Shock Wave Compacted 3Nb:1Ge Powder Mixtures.
- TABLE 5. Peak Pressures for Commonly Used Explosives.

PREFACE

This Final Report contains the results of work performed during the period of June 28, 1973 to August 15, 1974 under contract NAS8-30244, entitled "The Effect of Shock Wave Compaction on the Transition Temperatures of Al5 Structure Superconductors".

The research program was sponsored by the Advanced Research Projects Agency of the DOD, Washington, D. C., and administered by the NASA/Marshall Space Flight Center, Huntsville, Alabama. Dr. E. W. Urban and Dr. L. L. Lacy were the Contracting Officers' Representatives.

ABSTRACT

Several superconductors with the A 15 structure exhibit a positive pressure coefficient, indicating that their transition temperatures increase with applied pressure. Powders of the composition Nb_3Al , Nb_3Ge , $\text{Nb}_3(\text{Al}_{0.75}\text{Ge}_{0.25})$, and V_3Si have been compacted by explosive shock waves. The superconducting properties of these materials have been measured before and after compaction and it is found that regardless of the sign of the pressure coefficient, the transition temperature is always lowered. The decrease in transition temperature is associated with a decrease in the particle diameter.

The shock wave passage through a 3Nb:1Ge powder mixture leads to the formation of at least one compound (probably Nb_5Ge_3). However, the formation of the A15 compound Nb_3Ge is not observed. Elemental niobium powder can be compacted by converging shock waves close to the expected value of the bulk density. Under special circumstances a partial remelting in the center of the sample is observed.

I. INTRODUCTION

The intermetallic compound Nb_3Ge with the A15-type crystal structure was reported [1] to exhibit the highest known superconducting transition temperature (T_c) of 23.2 K. For these high- T_c materials the observation is generally made that the transition temperatures of superconductors with the A15 structure are not a priori optimum after they have been synthesized by the processes of melting, sintering, diffusion, sputtering or vapor deposition. In many cases, the T_c instead is reduced as much as several degrees Kelvin by such effects as lattice disorder [2], nonstoichiometry [3], lattice instability [4], or the existence of multiple phases [5]. These parameters have to be varied in order to optimize the superconductor for its maximum transition temperature. The importance of these effects has been demonstrated for several material systems as illustrated by the following examples: The crystallographic long range order in V_3Au was increased by annealing, and it was found that T_c could be raised from 0.015 to 3.22 K [6]. The intermetallic compound Nb_3Ge becomes superconducting at 23 K, but only when the stoichiometric composition is preserved at room temperature [1]; otherwise, its T_c is 6 K. Some A15 materials, especially those pseudo-binary compounds which contain V_3Si , exhibit an increase in the bulk transition temperature when a residual strain is preserved [7].

In order to be able to control and optimize those important parameters, new annealing, quenching and manufacturing techniques have to be applied. We proposed to investigate in A15 superconductors the influence of shock waves on those parameters, as reflected primarily by the transition temperature. The energy of a converging shock wave (or pressure pulse) has

been used recently to form the compound Nb_3Sn from its elemental powders [8]. It has been shown [9] that by this technique temperatures as high as 2000 °C and pressures in the range of 100 kbar can be obtained for the duration of approximately one micro-second. After passage of the shock wave the high pressure conditions are immediately released and, therefore, the sample is recovered in a practically quenched state. The application of the shock wave compaction technique on pre-reacted compound powders should result in a uniform compaction of the Al5 material, freeze in part of the pressure by the quenching effect, and possibly remelt some of the pulverized material.

Of particular interest was the compound V_3Si . It has been shown by Smith [10] that this material has a very large positive pressure coefficient of $\Delta T_c / \Delta p = 3.1 \times 10^{-2}$ K/kbar from which a theoretical increase in the transition temperature of 3.1 K is expected when the material is subjected to a uniform pressure of 100 kbar. The same positive pressure effect is found for Nb_3Au [11], but the pressure coefficient is ten times less than that for V_3Si . Other literature indicates [12] that the pressure coefficient for all the other listed materials may be negative in sign.

We have explosively compacted powders of Nb, Nb_3Al , Nb_3Ge , $\text{Nb}_3(\text{Al,Ge})$, and V_3Si and will report on the nature of the compaction process for these materials. In addition, the transition temperatures of the superconductors were measured before and after the compaction to ascertain the degree of frozen-in pressure caused by the shock wave passage through the superconductor.

II. SAMPLE PREPARATION AND PROCESSING

1. Cast Specimens

The task required the casting of the intermetallic compounds Nb_3Al , $\text{Nb}_3(\text{Al}_{0.75}\text{Ge}_{0.25})$, Nb_3Ge , and V_3Si from its elemental constituents. Most of the cast samples were prepared in the Ceramics Division of the Oak Ridge National Laboratory. An arc furnace [13] with water-cooled crucible and tungsten electrode was used to melt the mixed and die-compacted powders. The ingots obtained were remelted one more time to ensure homogenization. The furnace was flushed before every melting procedure with 99.99% pure argon. Mass losses were kept small and did not exceed 0.7 w.% for any specimen. Evaporation of aluminum, silicon, and germanium was observed but - besides the splattering of liquid droplets - did account for only a small amount of the total losses. The losses, if they had occurred by the evaporation of Al alone, would shift the composition for Nb_3Al by a maximum of 1.9 at .%. No correction for this anticipated small shift in composition has been made. Some typical weights of the specimens during processing are given in Table 1.

Annealing of the specimens was done in evacuated quartz tubes at 800°C for 10 hrs in the case of Nb_3Al , at 750°C for 100 hrs in the case of $\text{Nb}_3(\text{Al},\text{Ge})$, and at 1000°C for 1 hr in the case of V_3Si . As expected [14], the heat treatment increased the T_c by 1.0 K for Nb_3Al samples and by 1.15 K for $\text{Nb}_3(\text{Al},\text{Ge})$ samples as seen from Figure 1. There was no change beyond 0.1 K in T_c by annealing of V_3Si . The lattice constants listed in Table 1 were calculated from Debye-Scherrer diffraction rings using high angle reflections. They are accurate to $\pm 0.002 \text{ \AA}$. Annealing had no measurable effect on the lattice constant but increased the line intensities and their sharpness.

Table 1

Selected Data for Cast Compound Specimens

Composition	$\text{Nb}_3(\text{Al}, \text{Ge})^*$	$\text{Nb}_3(\text{Al}, \text{Ge})^*$	Nb_3Al	Nb_3Al	V_3Si
Catalog-Number	11	12	13	14	20
Weight of Cast Specimen (g)	15.6	15.7	12.4	12.0	17.0
Loss during Melting (g)	0.11	0.08	0.09	0.07	--
T_c (K) R.M. As Cast Cond.	18.79	18.73	17.33	17.31	16.30
T_c (K) R.M. Annealed Cond.	19.96	19.94	18.30	18.30	--
T_c (K) I.M. Annealed Cond.	19.82	19.80	18.26	18.27	16.1
Lattice Constant $(\text{\AA})^0$ Annealed Cond.	5.171	--	5.189	--	--
Annealing Conditions					
Temperature ($^{\circ}\text{C}$)	750	750	800	800	1000
Duration (hrs.)	100	100	10	10	1

*Exact net composition: $\text{Nb}_3(\text{Al}_{0.75}\text{Ge}_{0.25})$ T_c is taken as half-point of inductance or resistance change

R. M.: Resistance Measurement

I. M.: Inductance Measurement

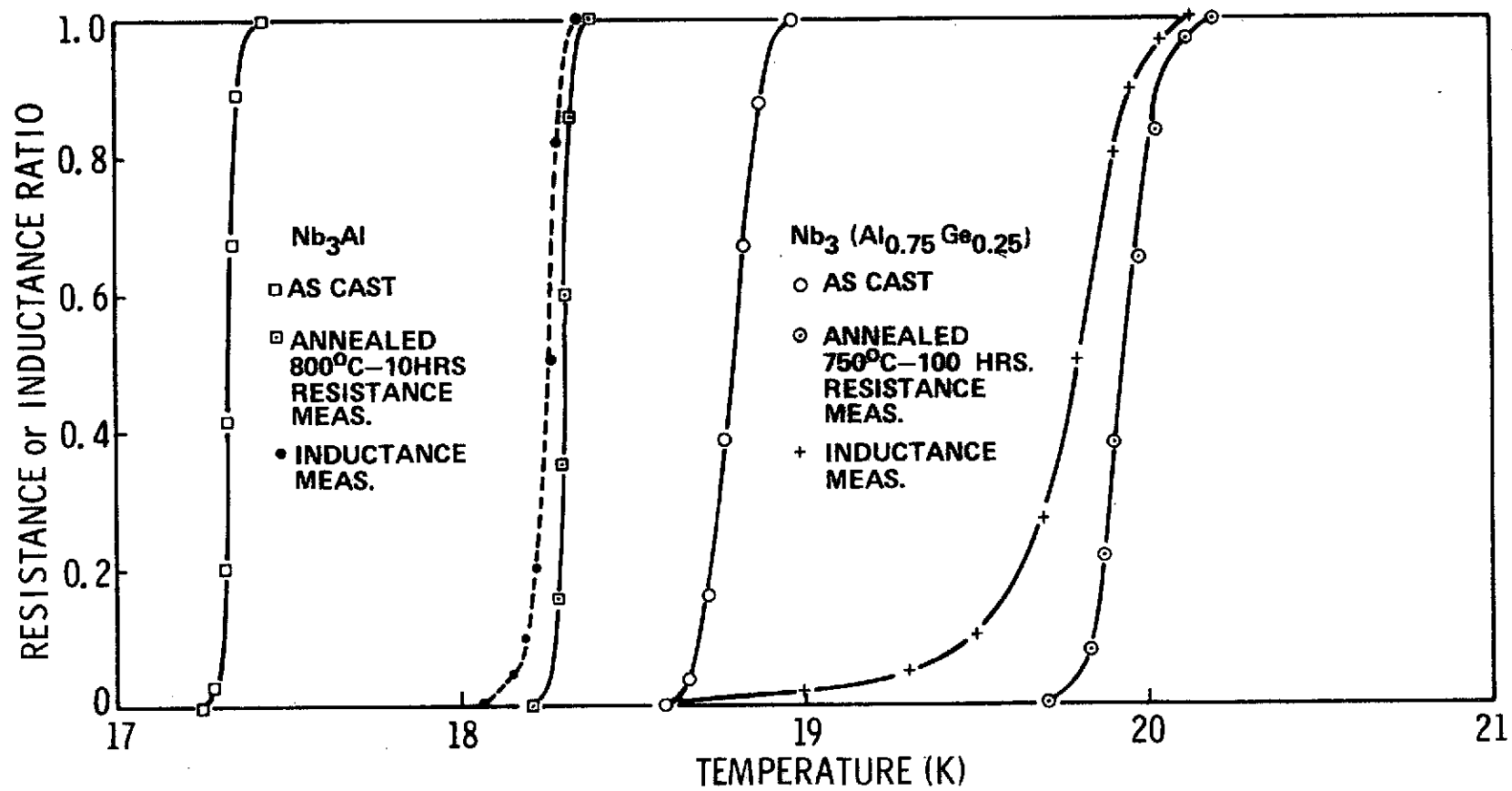


Figure 1. Transition curves of Nb_3Al and $\text{Nb}_3(\text{Al}, \text{Ge})$ cast samples.

2. Pulverization

To obtain the compound powders, cast ingots with the composition Nb_3Al , $\text{Nb}_3(\text{Al},\text{Ge})^*$, $\text{Nb}_3(\text{Al},\text{Ge},\text{Si})^{**}$, and V_3Si in the annealed state were crushed in a porcelain mortar at room temperature. The specimens appeared very brittle and crushed easily. Normally, two kinds of powders were obtained by sifting through standard 70 and 100 mesh sifts:

- i Powders with a grain size between 70 and 100 mesh, equivalent to a particle size between 150 and 210 μm . Grains of such a V_3Si powder are shown in Figure 12a.
- ii Powders with a grain size greater than 100 mesh, equivalent to a particle size of 150 μm and smaller.

These powders were filled separately in copper-tubes of 4.8 mm diameter and the powder density obtained was approximately half of the bulk density. To avoid contamination by oxygen or nitrogen the samples were purged with gaseous helium for at least 3 hours prior to sealing. The superconducting transition temperature of these uncompacted powders was measured by the inductance technique and the results are reported with those of the bulk materials in Section III, 2.

* Exact net composition: $\text{Nb}_3(\text{Al}_{0.75}\text{Ge}_{0.25})$

** Exact net composition: $\text{Nb}_3(\text{Al}_{0.75}\text{Ge}_{0.01}\text{Si}_{0.24})$

3. Shock Wave Generation

For all shock wave compaction experiments the explosive nitroguanidine [$\text{NH}_2\text{-C(NH)-NHNO}_2$] has been used. The detonation velocity of this material is with 3.5 km/sec somewhat lower than that for the well-known explosive TNT (Trinitrotoluene), but the advantage of using nitroguanidine is that it can be packed safely with variable density. Thus a variation in the detonation velocity and shock pressure is achieved. The samples were inserted centrally into cylindrical containers packed with the explosive. Figure 2 shows the arrangement [15] in a schematic fashion. In order to assure a homogeneous shock wave formation across the entire length of the sample, the top end of the sample and the detonator were kept 3 cm apart. The shock wave initiation was accomplished with an electrical detonator and tetryl booster cap positioned centrally on top of the container. By this technique, a cone shaped converging pressure pulse is focussed by oblique reflection on the symmetry axis of the set-up, which is the sample center and the pressure pulse travels the entire length of the sample. As the ductile copper jacket collapses, the powder is subjected to an extensive compaction. Due to the chosen geometry, an increasing pressure is generated towards the center of the sample. The shock pressure could be varied by changing the density of the explosive charge which affects the burning velocity of the nitroguanidine or by changing the size of the container. Two standard sizes have been used with the following dimensions: 12.5 cm diameter and 16 cm high ($1,960 \text{ cm}^3$) or 15.2 cm diameter and 17.1 cm high ($3,100 \text{ cm}^3$).

A third method to increase the shock pressure is the following:

Rather than igniting the explosive charge from a point source which creates the covering shock wave by oblique reflection, a simultaneous

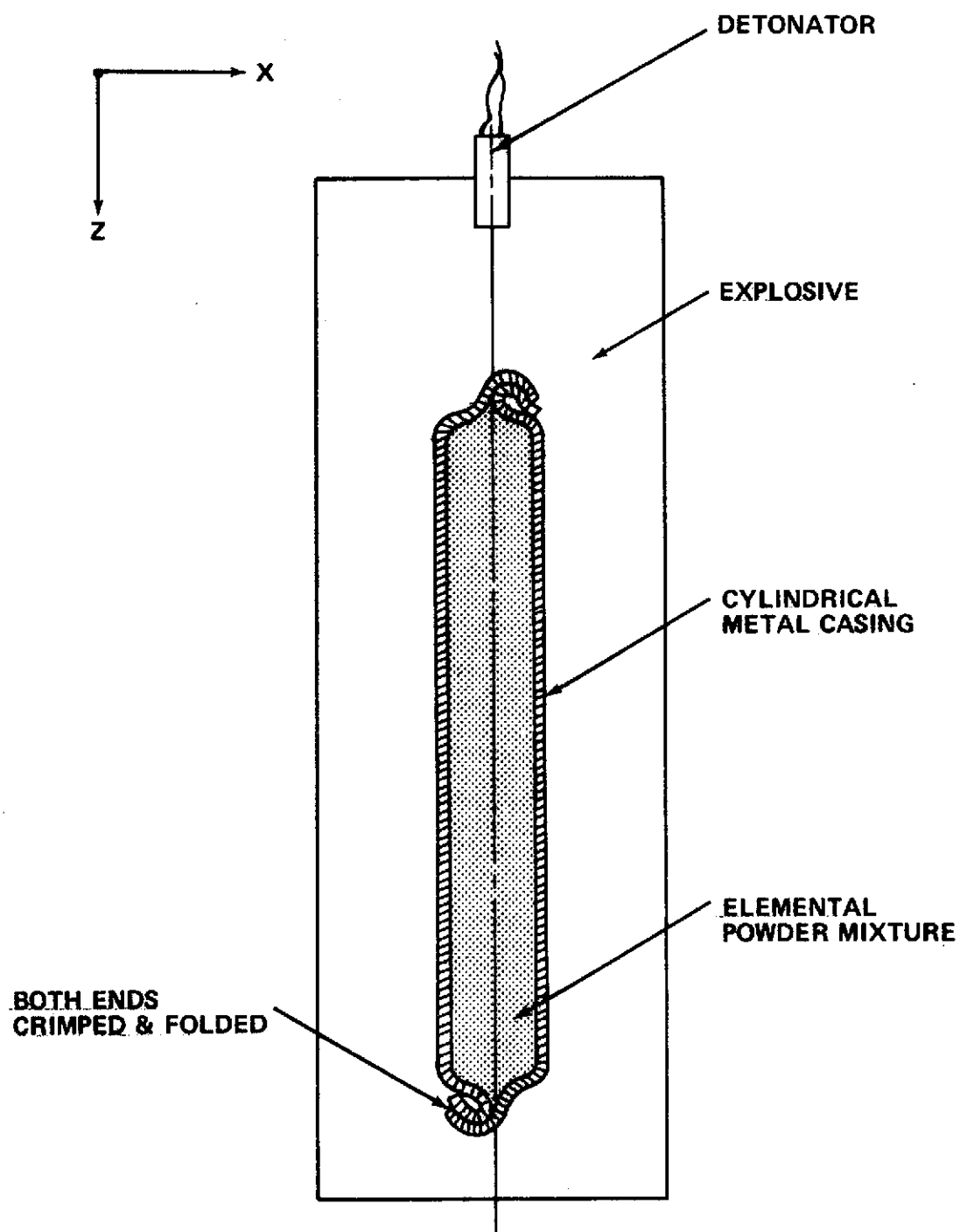


Figure 2: Schematic representation of the converging shock wave technique for powder compaction.

ignition of the nitroguanidine along the outer circumference was achieved by using a line wave generator. This triangular shaped thin sheet of explosive, with small holes punched in to properly delay the shock wave, is ignited with a point source on top and generates a linearly progressing wave front at the baseline. By this modification, two primary shock waves collide in the sample and the shock pressure can be further increased. Prior experience gained from the preparation of the compound Nb_3Sn from niobium and tin powders [9] indicated that a hole was always formed in the center of the sample by application of this modification. On the contrary, no hole formation was observed when compacting powders of cast samples with this technique. Considerations about the shock wave propagation in this symmetrical set-up are given in Section IV.

4. Low Temperature Set-up

The transition temperatures of the compound materials before and after shock wave compaction were measured by the flux expulsion technique (inductance measurement). The advantage of this method, in addition to its high sensitivity, is that under special circumstances the volume of the material becoming superconducting can be determined. A schematic of the experimental setup is given in Figure 3. The sample is placed inside a coil with an inductance of approximately 1 mH, and the inductance is measured with a bridge circuit. The material becoming superconducting exhibits diamagnetism and so excludes the magnetic flux from its volume. When this happens, the inductance of the coil changes and the bridge circuit becomes unbalanced. In order to increase the sensitivity of the system and to reduce susceptibility to noise, the a-c signal is detected with a lock-in amplifier. The temperature of the sample is measured with a calibrated germanium resistor. The resulting signals for both temperature and inductance are recorded on a x-y recorder.

In several cases the transition temperature was also determined by the resistive technique (Figure 4) measuring the voltage drop across a certain portion of the material as a function of temperature. Because of the high resistivity of the investigated materials ($100 \mu\Omega \text{ cm}$), a current of 20-30 mA was sufficient to generate an appreciable voltage drop. Only the highest T_c will be picked up in the event that the material is multiphase with different transition temperatures. Electrical contacts were made with silver conductive paint. The transition temperature (T_c) is defined as that temperature where the inductance or resistance change reaches half of the total change.

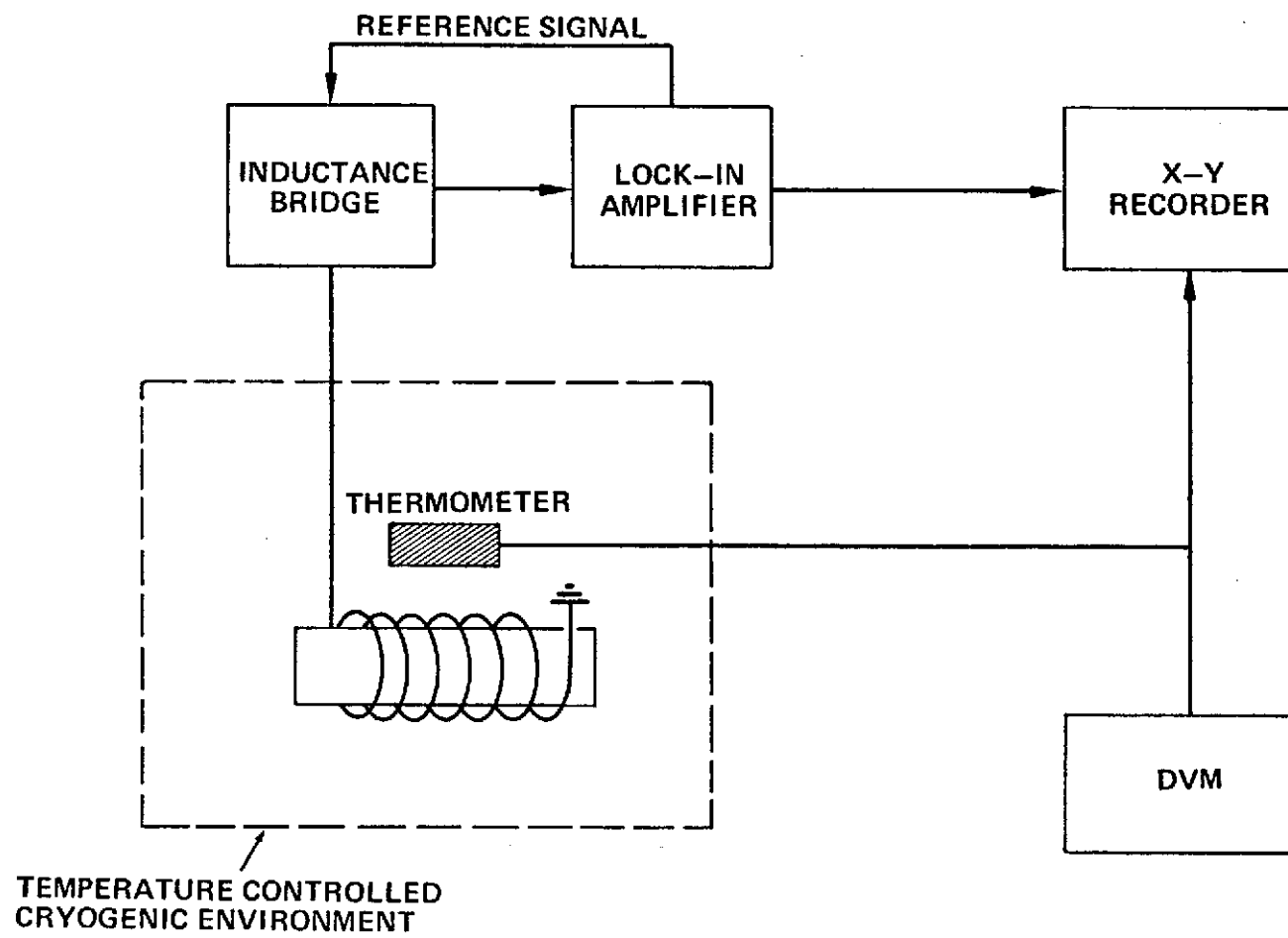


Figure 3: Block diagram for resistive measurement of T_c .

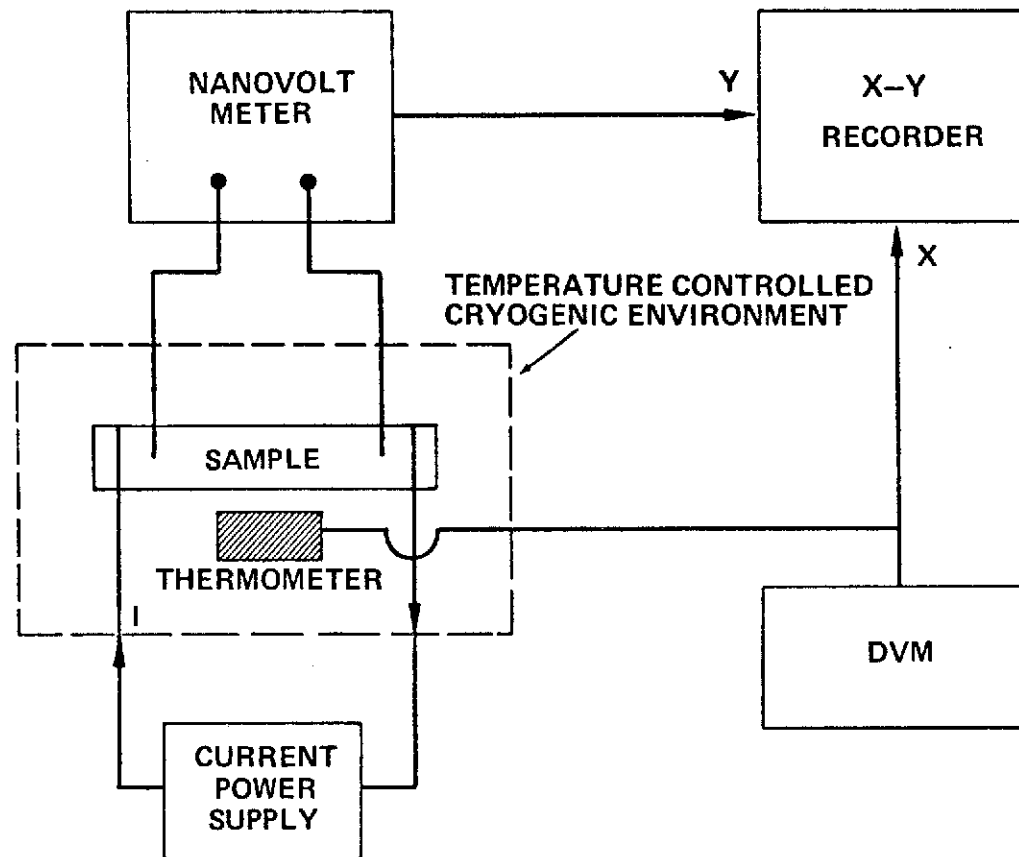


Figure 4: Block diagram for resistive measurement of T_c .

5. Optical, X-ray, and Microprobe Analysis

Information about the appearance and structure of the samples was gained by optical microscopy. The compacted samples polished without difficulty; however, some particles broke loose during the polishing process indicating a higher than actual degree of porosity.

X-ray Debye-Scherrer deflection measurements on selected specimens were made in a standard powder diffraction camera with 57.3 mm diameter using CuK_α radiation.

The scanning electron micrographs and X-ray microprobe analyses were performed with standard equipment. So far, no microprobe analyses have been performed on shock compacted A15 powders.

III. EXPERIMENTAL RESULTS

1. Appearance of Compacted Compound Powders

Nine different samples, containing the pulverized compounds Nb_3Al , $\text{Nb}_3(\text{Al}_{.75}\text{Ge}_{.25})$, V_3Si , and $\text{Nb}_3(\text{Al,Ge,Si})$ have been subjected to the shock wave compaction process. Since no prior experience was available as to the effect of this compaction process on the properties of the compounds, the optimum conditions in regard to the maximum transition temperature with the formation of Nb_3Sn from Nb and Sn powders were chosen [8,9]. A local analysis of the compacted powders showed that degree of compaction was homogeneous along the length of the sample and no macroscopic voids were apparent.

The degree of compaction was so high that the density of the compacts is within 95% of the value for the bulk materials. The density of the starting powders was approximately half of the bulk density with the 70-100 mesh powder having a little higher packing density than the > 100 mesh powder.

Encouraged by these results, the explosive load for some of the samples was increased up to 0.55 g/cm^3 and even under the resulting severe shock pressures, estimated in excess of 100,000 bars, no formation of a central void was observed.

Whenever those shock wave conditions were applied to the formation of Nb_3Sn , a hole in the center of the sample ($\sim 1 \text{ mm}$ diameter) was formed. The composition of the selected compound materials, the grain size of the powders, and the applied explosive loads are listed in Table 2.

Table 2

Data for Shock Wave Compacted Compound Powders

Sample	Composition [†]	Grain Size (Mesh)	Explosive Load (g)	Density of NG (g/cm ³)	Remarks
52	Nb ₃ (Al,Ge)*	>100	1,050	0.53	LWG, cast #11
53	Nb ₃ (Al,Ge)*	70-100	1,060	0.53	
54	Nb ₃ (Al,Ge,Si)**	>100	1,620	0.52	LWG, cast #13
55	Nb (Al,Ge,Si)**	70-100	1,630	0.52	
51	V ₃ Si	70-100	1,080	0.55	
57	V ₃ Si	70-100	1,060	0.54	LCW,
56	V ₃ Si	>100	1,500	0.48	
70	Nb ₃ Al	>100	1,130	0.58	Not found
71	Nb ₃ Al	>100	1,080	0.55	LCW
2	Nb	325	1,130	0.43	See III, 4

NG Nitroguanidine

LWG Line Wave Generator used

+ All samples in annealed state.

* Exact net composition: Nb₃(Al_{0.75}Ge_{0.25})

** Exact net composition: Nb₃(Al_{0.75}Ge_{0.01}Si_{0.24})

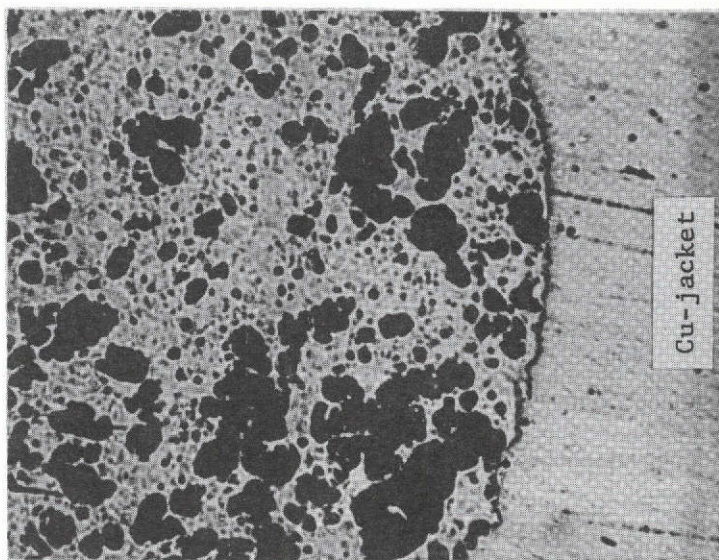
Photomicrographs on unetched surfaces of shock compacted $\text{Nb}_3(\text{Al,Ge,Si})$ are shown in Figure 5. The dark spots represent void areas which may have been caused by the loss of particles during the polishing process. Photomicrographs on etched surfaces taken in the center portion of a shock compacted V_3Si and $\text{Nb}_3(\text{Al,Ge})$ sample are given in Figure 6. Whereas the bulk V_3Si material appears mostly single phase, as seen from the photograph (Figure 6a), the $\text{Nb}_3(\text{Al, Ge})$ material was multiphase [3] with a large amount of $\alpha\text{-Nb}$ present (Figure 6b, shaded areas). The compaction has caused extensive cracks throughout the material.

2. Superconductivity of Compacted Compound Powders

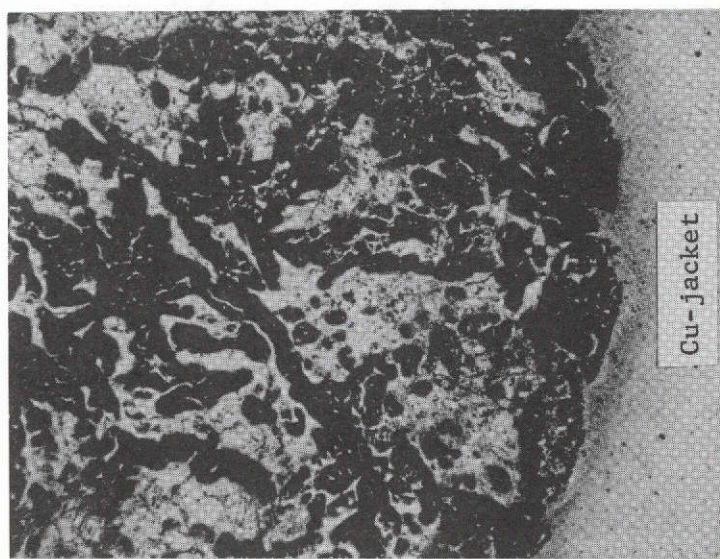
Superconducting transition curves of the compounds before pulverization and shock wave compaction were generated using the flux-expulsion technique which measures the change in inductance of a coil. The change in inductance when the sample went from the normal to the superconducting state ($\Delta L/L$) was around 1% for the amount of material used. For the transition curves, the normalized change in inductance was plotted as a function of temperature. For this procedure all samples were assumed superconducting at 8 K, since the induction did not change below this temperature. In order to obtain reproducible results on the low temperature measurements, it was necessary to remove the copper jacket from the compacted samples. This was achieved by machining the copper away for a length of approximately 1 cm from the cylindrically shaped core.

a. $\text{Nb}_3(\text{Al}_{0.75}\text{Ge}_{0.25})$

The transition curves of the compound material $\text{Nb}_3(\text{Al,Ge})$ in its various stages of processing are shown in Figure 1. The bulk compound after annealing at 750°C for several hours had a transition temperature of



Sample #54 $\text{Nb}_3(\text{Al,Ge,Si})$ 50X



Sample #57 V_3Si 50X

Fig. 5: Photomicrographs of shock wave compacted compound powders.

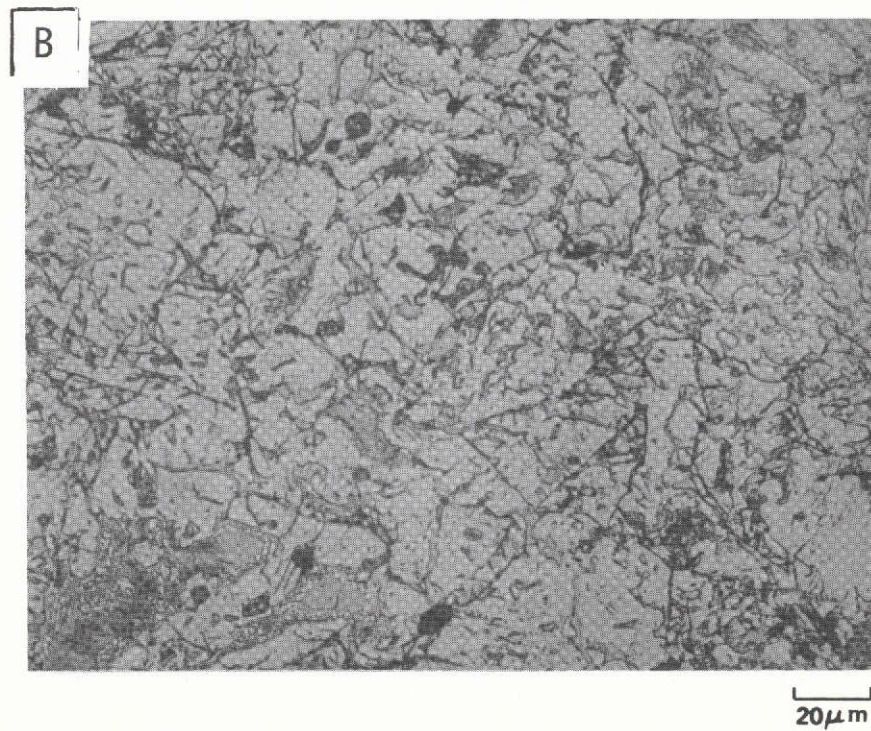
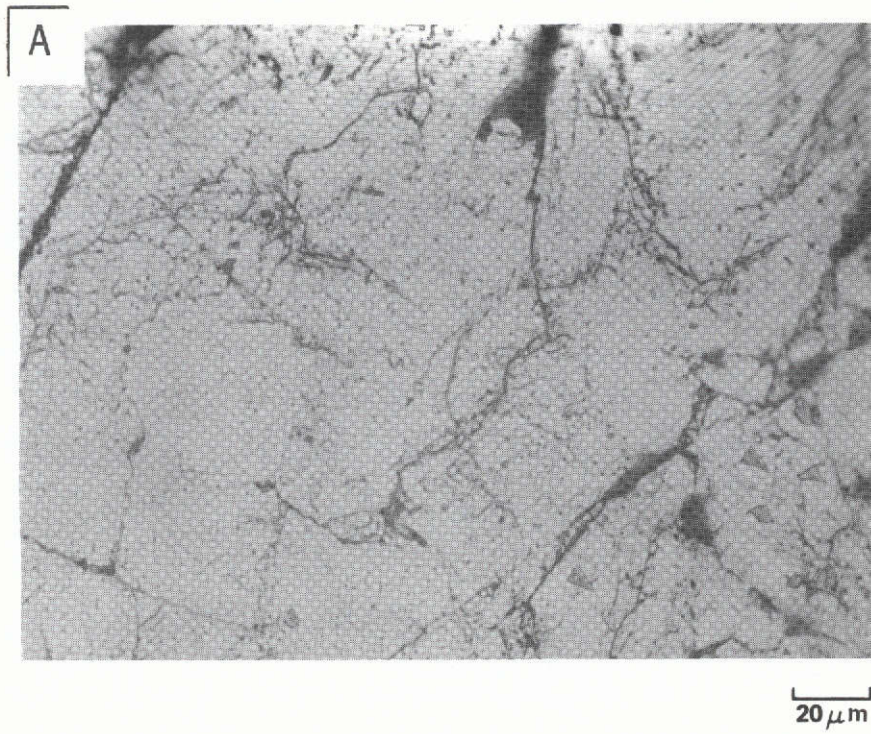


Figure 6: Photomicrographs (etched) of shock wave compacted compound powders. 500 X
A. V_3Si (Sample #57) B. $Nb_3(Al,Ge)$ (Sample #52)

20.2 K with the onset of superconductivity occurring at 20.45 K. These data are in agreement with published results [14]. The sample used is not completely homogeneous in composition since the transition curve shows the appearance of a small tail section below 20 K., as can be seen in Figure 1. However, this tail section is not found when resistive measurements of the transition are made.

Pulverization of the Al₅ material to a grain size between 150 and 210 μm (70-100 mesh) changes the shape of the transition curve which is now spread over a range of more than 6 K. It can be seen that the onset temperature of the superconducting transition is left unchanged by the pulverization, but simultaneously, the tail section becomes more dominant. It is found that the powder with the smallest particle size has the most pronounced tail section and the largest transition width. Shock wave compaction of the powder further reduces its transition temperature as can also be seen in Figure 7.

Transition curves for the material Nb₃(Al,Ge,Si) are shown in Figure 8. The difference in composition of this sample to the Nb₃(Al,Ge) sample is that 96% of the germanium is substituted in this compound by silicon, resulting in a chemical composition of Nb₃(Al_{0.75}Ge_{0.01}Si_{0.24}). The apparent effect of the substitution of Ge by silicon is that the crystal structure stays unchanged, but the transition temperature is lowered without changing the shape of the transition curve. The effect of pulverization and shock wave compaction on the transition curves for the material Nb₃(Al,Ge,Si) is basically the same as found for Nb₃(Al_{0.75}Ge_{0.25}). This sample because of its high T_c had been chosen as a training material for the compaction.

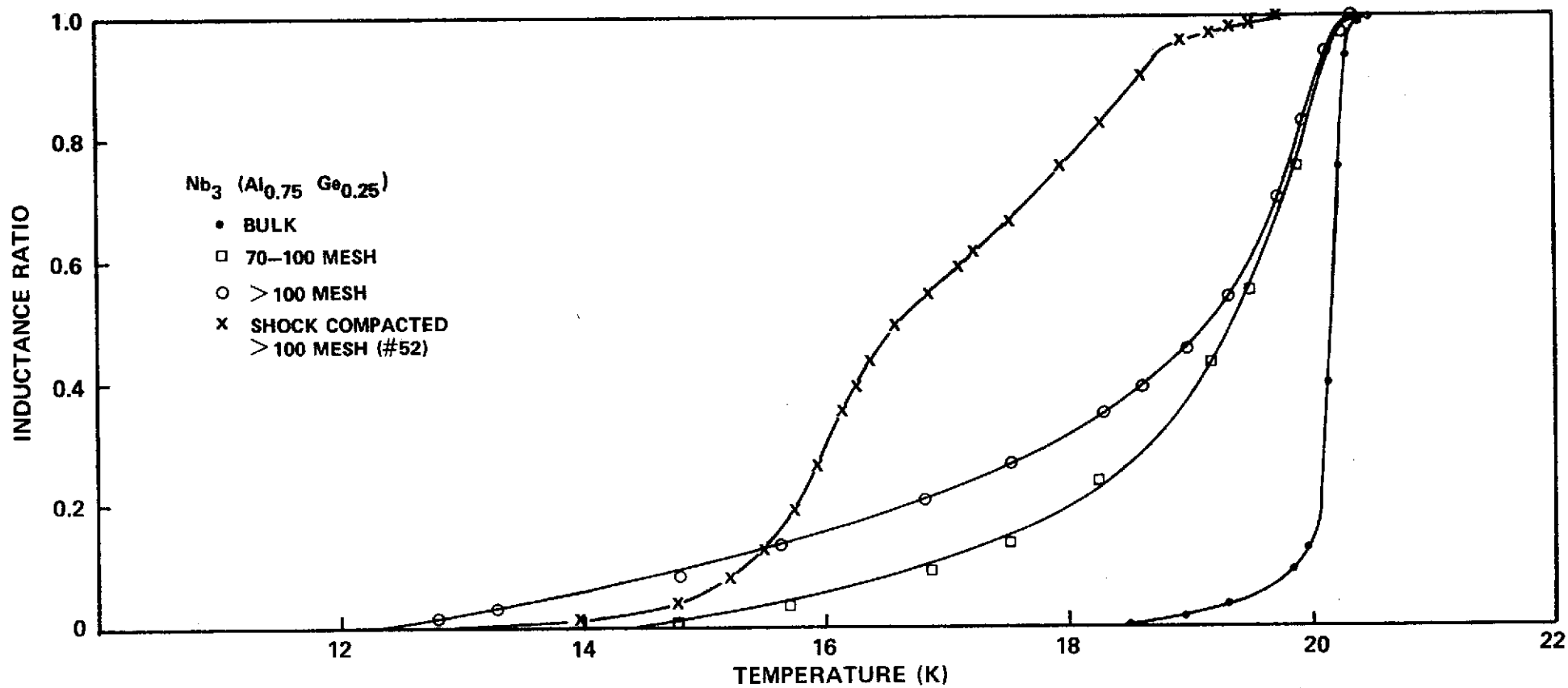


Figure 7: Superconducting transition curves for $\text{Nb}_3(\text{Al}_{0.75}\text{Ge}_{0.25})$ in bulk, pulverized, and shock compacted state.

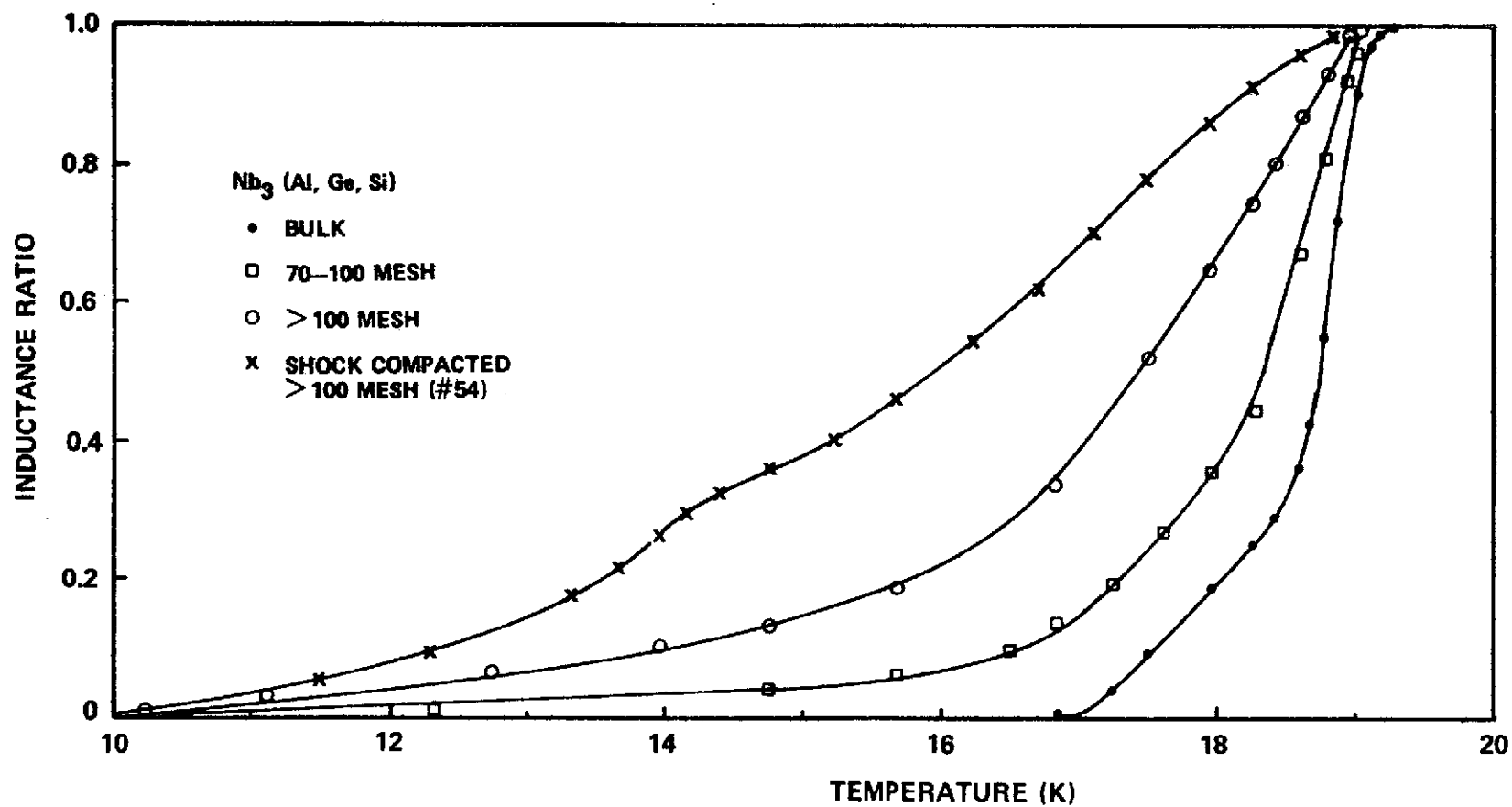


Figure 8: Superconducting transition curves for $\text{Nb}_3(\text{Al, Ge, Si})$ in bulk, pulverized, and shock compacted state.

b. Nb_3Al

Transition curves of Nb_3Al (annealed at 800°C), after pulverization, and after shock wave compaction are shown in Figure 9. The magnitude of the reduction in T_c is the same as found for the previously described materials. Again, the onset temperature of superconductivity is left unchanged by the pulverization and compaction processes. Since the materials $\text{Nb}_3(\text{Al},\text{Ge})$ and $\text{Nb}_3(\text{Al},\text{Ge},\text{Si})$ are all related to Nb_3Al in that a specific amount of Al in the Nb_3Al compound is substituted by Ge or Si, leaving the crystal structure unchanged, the observed changes in transition temperature may be those associated with Nb_3Al .

c. V_3Si

Transition curves for various V_3Si samples after pulverization and after shock wave compaction are shown in Figures 10 and 11. The bulk V_3Si material which was annealed at 900°C exhibits a rather sharp transition to the superconducting state at 16 K. This value is about 0.9 K below the temperature reported in the literature [16]. Since the T_c of V_3Si is very sensitive against small deviations from stoichiometry, the lower T_c observed for this sample may be caused by such deviations. Pulverization of the material surprisingly raises the onset-temperature for superconductivity to 17.1 K which value should have been found for the bulk material. The powder with a particle size between 150 and 210 μm appears to be a two phase material with two distinct transitions. The two transitions become less distinct for finer powders. Shock wave compaction of V_3Si powders further reduces their transition temperature as can be seen from Figures 10 and 11.

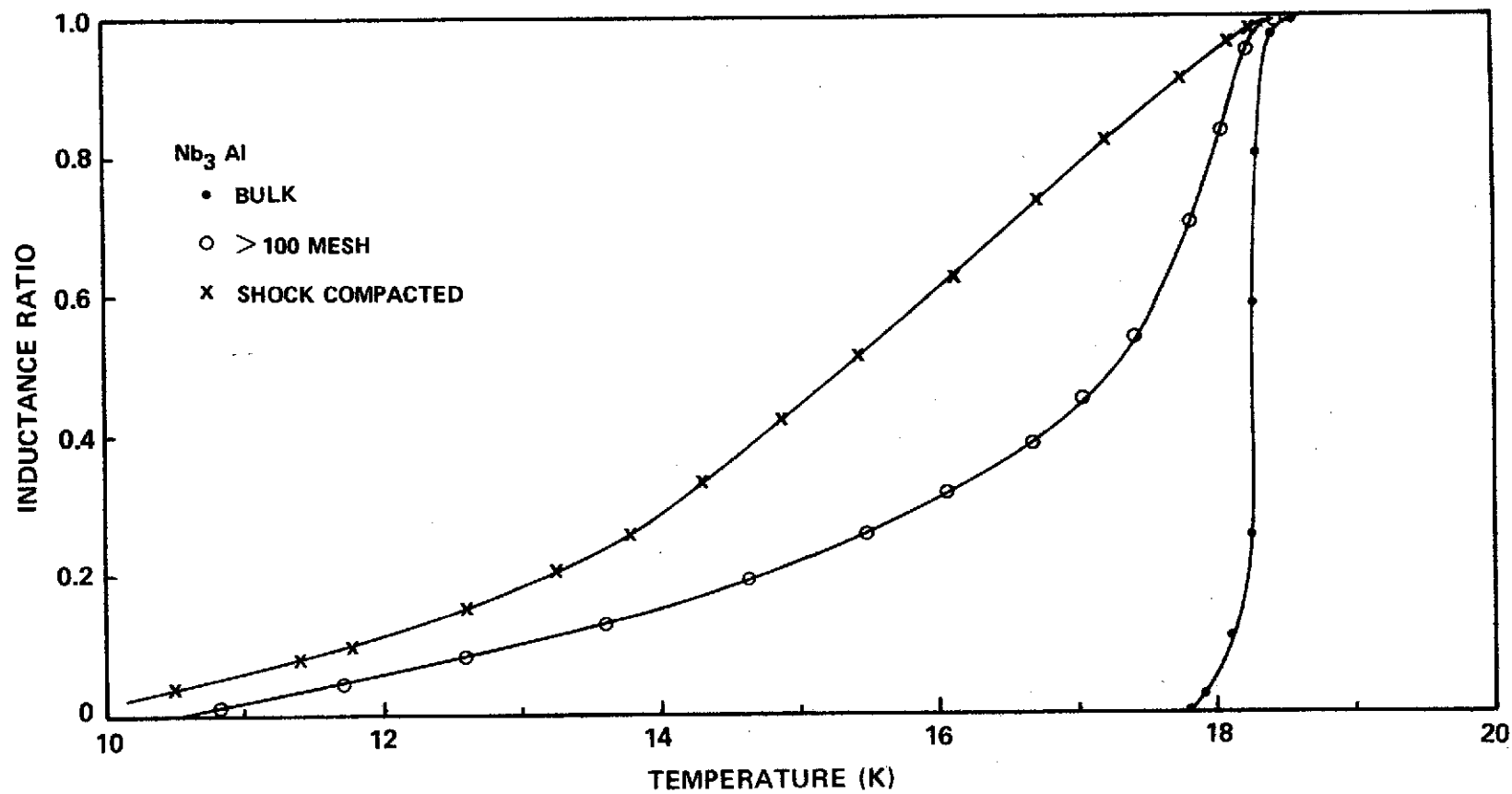


Figure 9: Superconducting transition curves for Nb₃Al in bulk and shock compacted state.

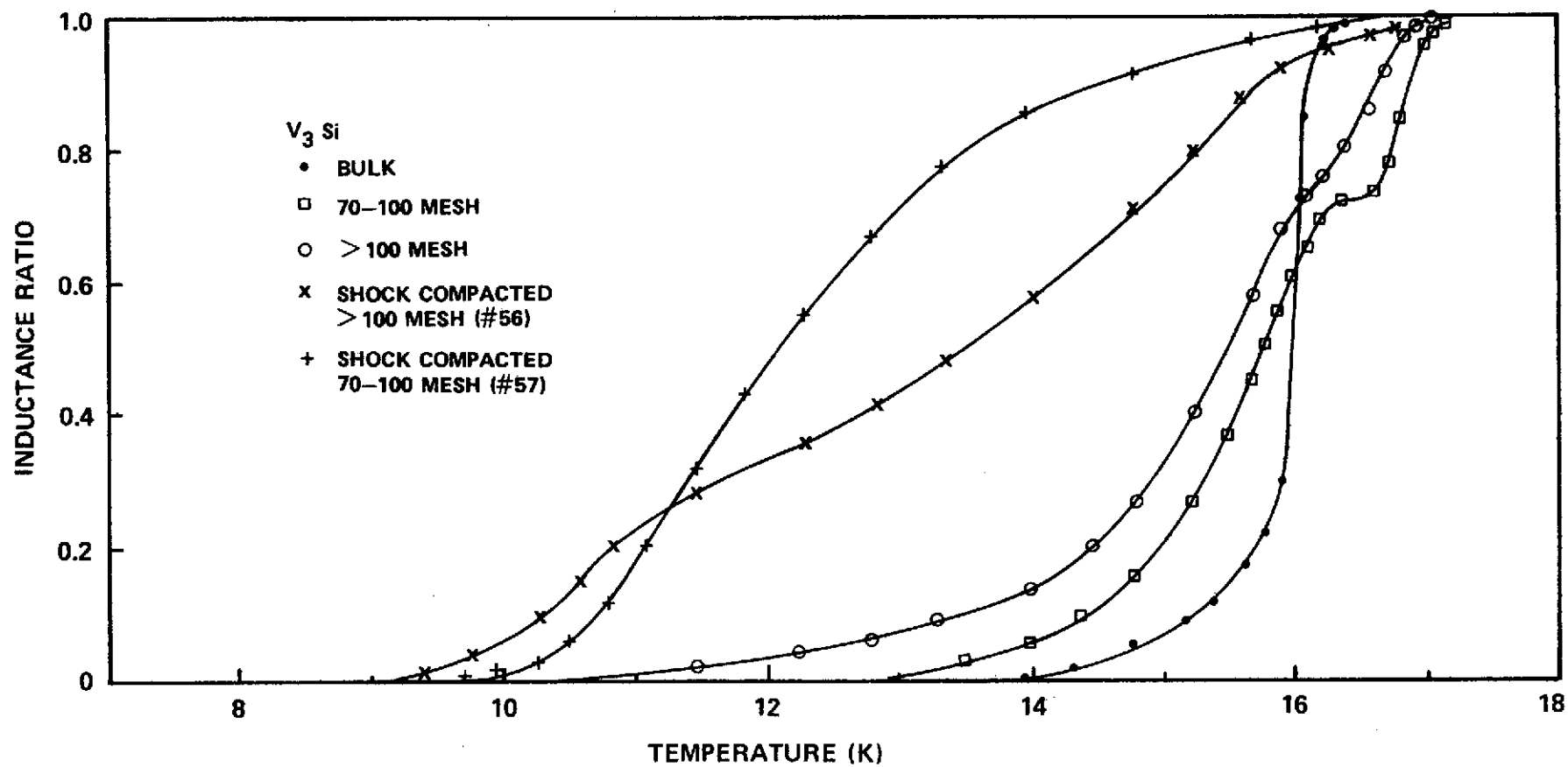


Figure 10: Superconducting transition curves for V_3Si in bulk, pulverized, and shock compacted state.

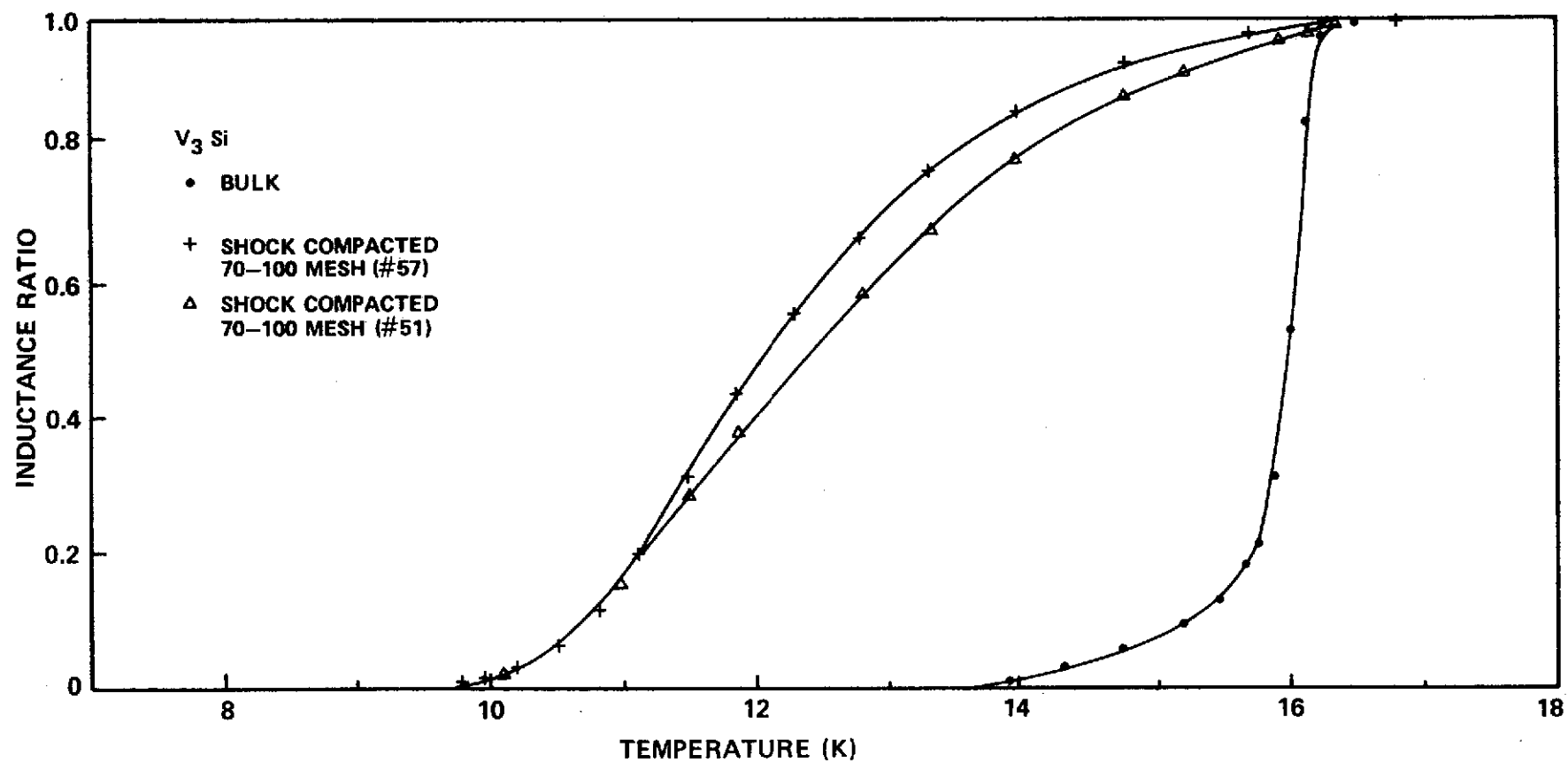


Figure 11: Superconducting transition curves for V_3Si in bulk, pulverized, and shock compacted state.

For all investigated compounds, it may be concluded that the shock wave compaction results in a reduction of the transition temperature by about 4.0 K when compared with the bulk T_c . Simultaneously the transition width is increased up to 6 K. At present it is not known if the reduction in T_c is related to a particle size effect or to a possible compositional inhomogeneity in the samples, uncovered by the inductive T_c measuring technique.

3. Microstructure of Compacted V_3Si

Since both the pulverization of the bulk material and the subsequent shock wave compaction resulted in a substantial decrease of T_c regardless of the superconducting pressure coefficient of the material, a study of the particle sizes in the shock compacted samples was initiated. For this purpose part of the compacted V_3Si sample (#57) was removed from its copper jacket and then transversally broken by hand. The circular break area was investigated with a scanning electron micrograph. Figure 12 shows in comparison with the same magnification the so-prepared cross-sectional area and some representative grains of the starting powder (diameter between 150 and 210 μm). It may be seen (from this figure) that the passing shock wave indeed greatly compacted the powders but also fractured each individual grain. A higher magnification of the outside area as well as the center area is shown in Figure 13a and b respectively. From the photographs it may be concluded that the fracturing occurs all over the sample cross-section but with less fracturing occurring in the center area. In the outer zone, particles well below a diameter of 3 μm can be observed. It is anticipated that the fracturing is responsible for the further decrease in the transition temperature. Since the T_c of V_3Si was not increased after the compaction, despite a positive pressure coefficient, it can be concluded

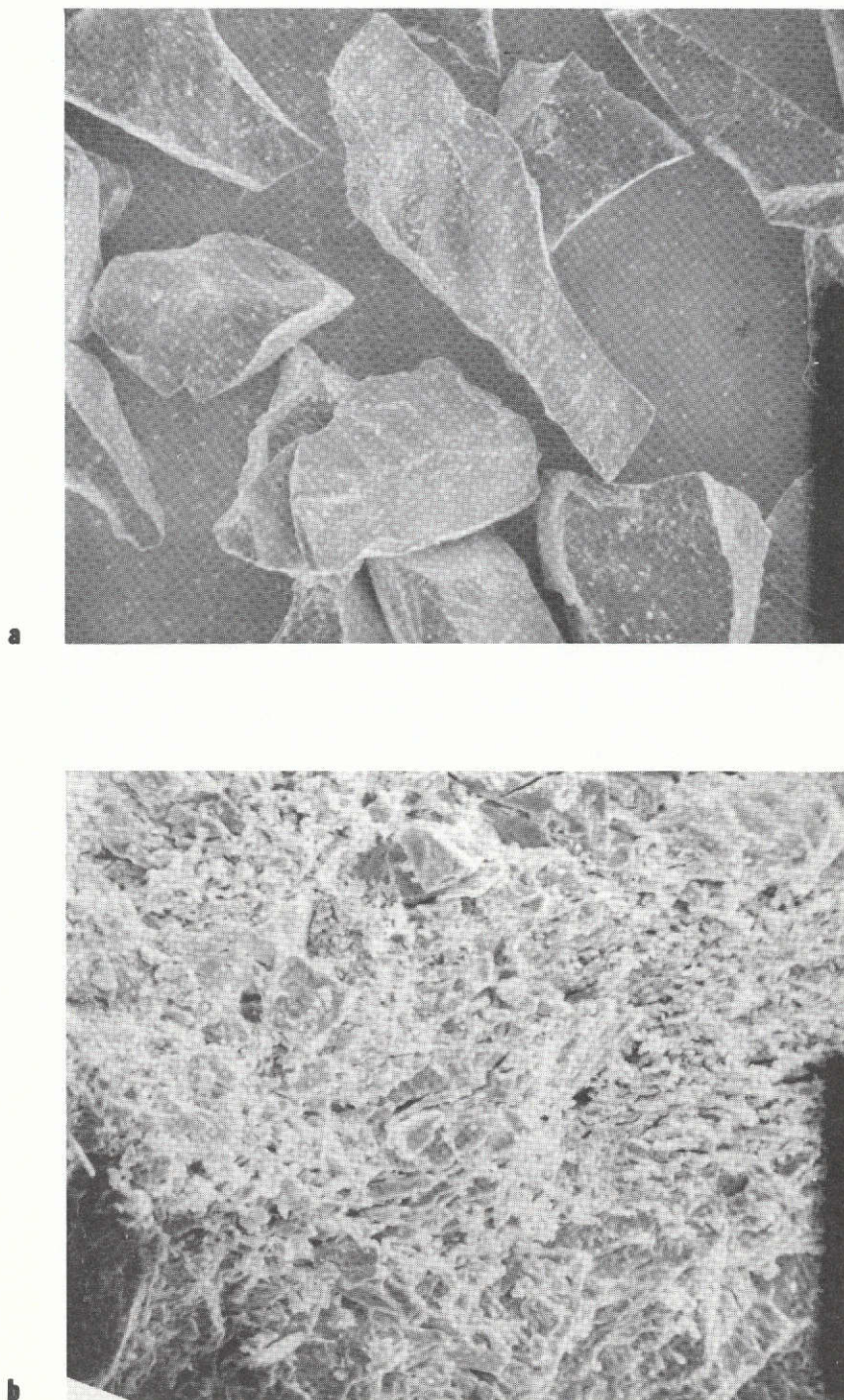


Figure 12: Scanning Electron Micrographs of V₃Si powder (#57), a) before and b) after shock wave compaction. Magnification: 100 X.

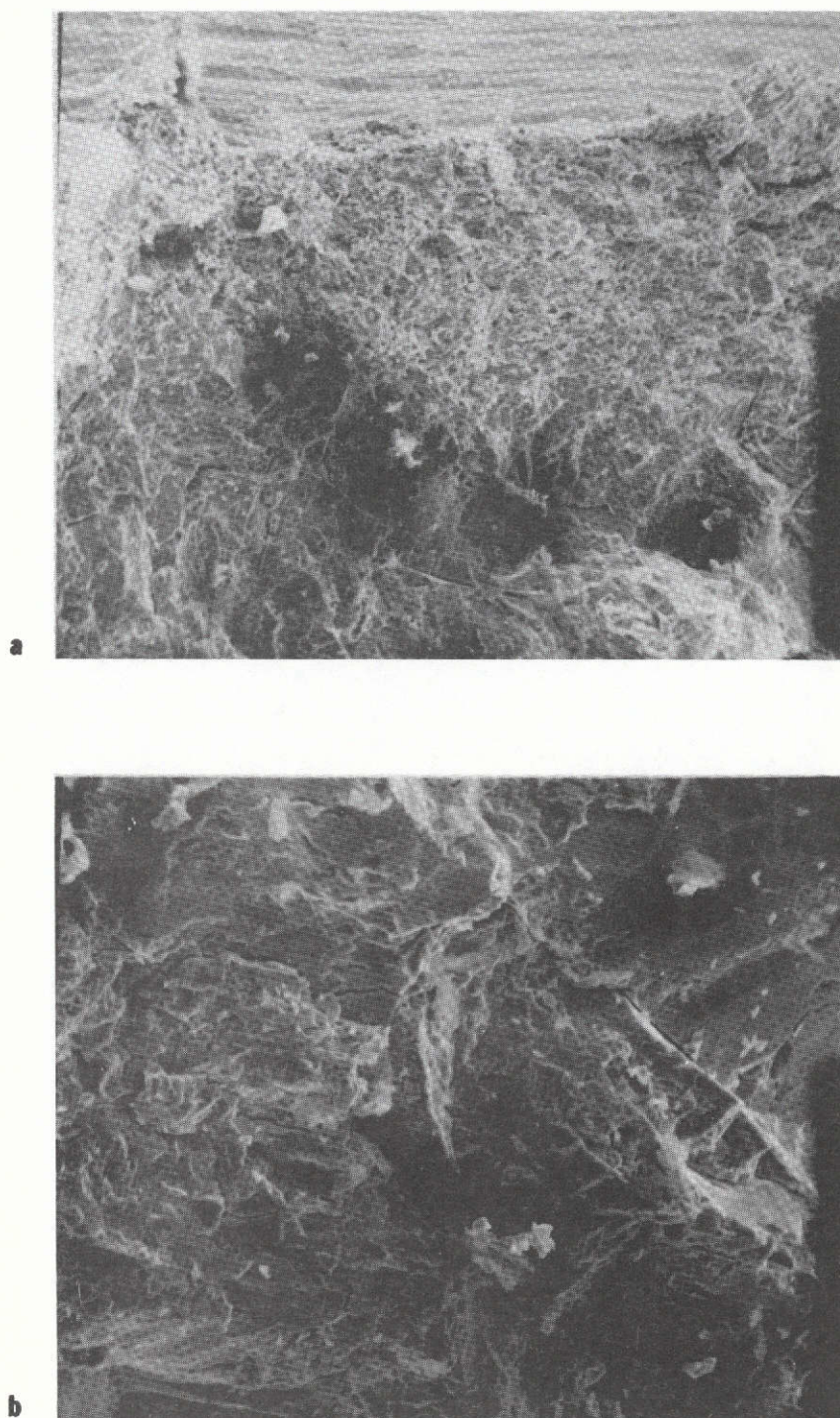


Figure 13: Scanning Electron Micrographs of V_3Si powder (#57) after shock wave compaction. a) outside area, b) center area. Mag.: 300 X.

that the amount of frozen-in uniform pressure is minimal. Due to the low compressibility of V_3Si , the energy of the converging shock wave was primarily used to fracture the material rather than to distort the lattice. A Debye-Scherrer analysis supports this conclusion with the high index lines becoming very diffuse and broad without noticeable change in the lattice constant (within 0.005 \AA).

4. Shock Wave Compaction of Pure Niobium Powder

Pure niobium powder with a particle size of 20 to 30 μm has also been compacted by shock waves. The parameters for generating the shock wave were the same as for the compaction of V_3Si with the only difference that the density of the explosive for Nb with 0.43 g/cm^3 was appreciably lower than that for V_3Si (0.54 g/cm^3). Photomicrographs of polished and etched cross-sections of one sample with different magnifications are given in Figure 14a and b. The appearance of a partial remelting of the niobium in the center can be observed. This remelting may be caused by the high compressibility exhibited by the niobium compared with the very low compressibility for V_3Si . The measured density for the compacted Nb powder was 97% of the theoretical density. No grain fracturing after the compaction is recognized.

Data for three different samples compacted with slightly different shock wave parameters are given in Table 3. It may be seen that the superconducting transition temperature of the niobium after compaction is also decreased by at least 1.2 K. Debye-Scherrer X-ray patterns taken from the shocked specimens showed line broadening which increased with the angle of deflection. Therefore, no exact values for the lattice parameter can be given, but it can be concluded that the lattice constant did not change within 0.01 \AA compared with the value for the starting powder.

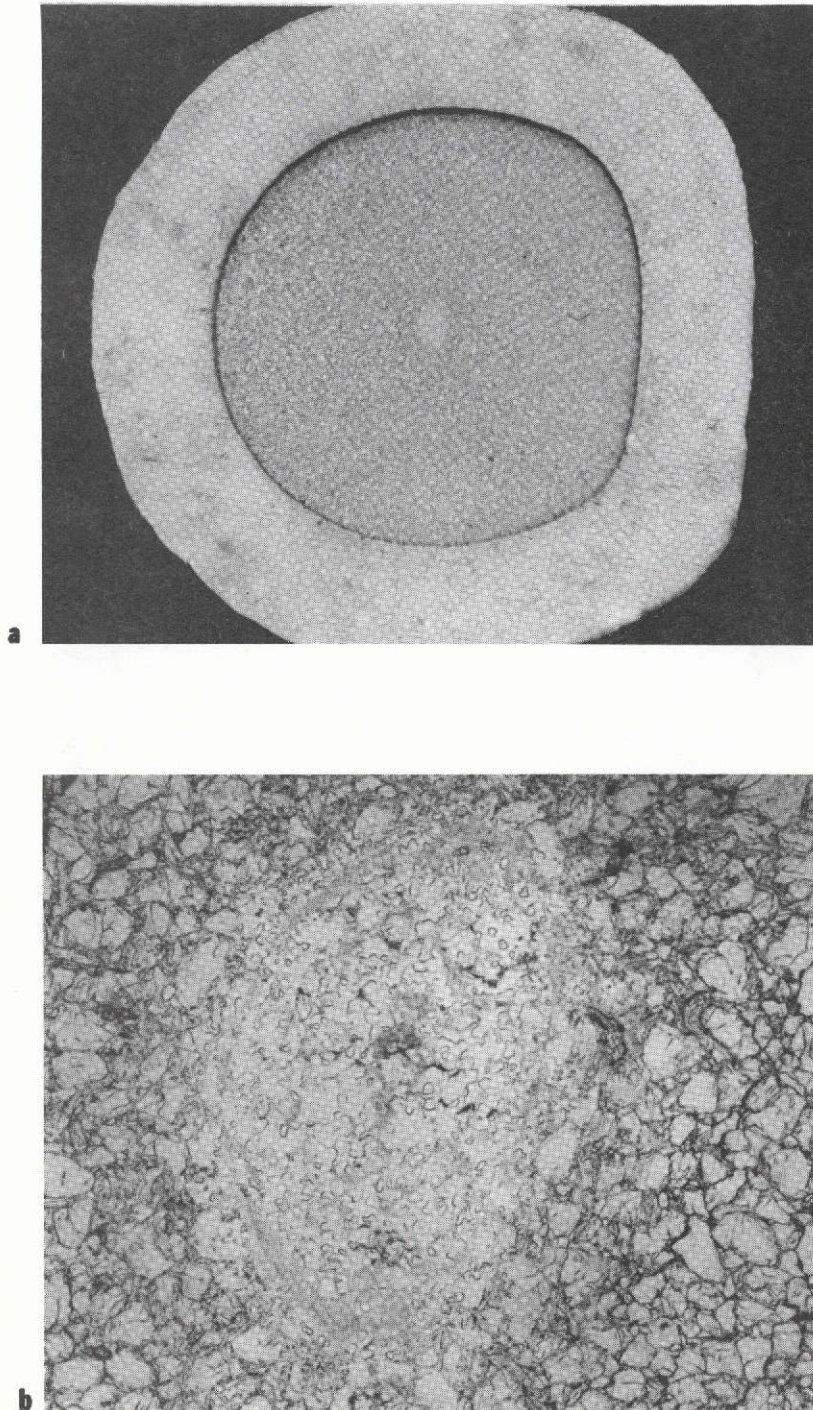


Figure 14: Shock compacted niobium powder with central remelt area.
Etched surface. Magnification: a) 15 X, b) 200 X.

Table 3

Properties of Shock Compacted Niobium Powder

Sample No.	Density of explosive (g/cm ³)	Density of compacted powder (g/cm ³)	Achieved density (%)	T _c (K) (Half Point)	Transition width ΔT(K)	Lattice constant a (Å)
0	uncompacted	-----	-----	9.2	0.05	3.306 ± 0.002
10	0.30	8.07	94	8.1	0.06	3.306 ± 0.01
1	0.42	8.13	95	7.75	0.08	3.306 ± 0.01
2	0.44	8.30	97	7.8	0.14	3.306 ± 0.01
Cast Nb	-----	8.57	100	9.3	0.02	3.300 ± 0.002

5. Attempted Synthesis of Nb_3Ge from its Constituents

The "Symposium on Superconductivity and Lattice Instabilities" was held in Gatlinburg, Tennessee, from September 10 - 12, 1973. One significant result of the conference in respect to the objectives of this contract was the report of superconducting Nb_3Ge films by J. R. Gavaler [17] with the very high transition temperature of 22.3 K. An even higher transition temperature of 23.2 K - but so far not reproduced - was measured by L. R. Testardi [18]. Relying on these presentations, the synthesis of Nb_3Ge by the shock wave compaction technique from niobium and germanium powders was initiated. Four samples have been prepared and investigated.

For all $3\text{Nb}:1\text{Ge}$ samples, high purity niobium (99.9%) and germanium (99.99%) powders with a grain size of -325 mesh were used as the starting materials. The powders were weighed to correspond to the chemical composition Nb_3Ge . The mechanically mixed materials were filled in ductile copper tubes of 4.8 or 6.2 mm diameter and 0.8 mm wall thickness and purged with gaseous helium for at least 10 hours prior to sealing the tubes by crimping their ends. After this procedure, the samples were approximately 12 cm long. Data of the compaction parameters are given in Table 4. Low temperature resistance measurements on the shocked specimens with the copper jacket still attached show no discontinuity within 1% in the temperature dependence of the electrical resistance which would indicate the existence of the high T_c compound. However, the formation of one or more intermetallic compounds of so far unknown composition in the center of the specimens is established. This can be concluded from the hardness of the core which is much greater than that of the outside area. A summary of the data obtained on the four samples is given in Table 4.

Table 4

Data for Shock Wave Compacted 3Nb:1Ge Powder Mixtures

Sample	#1	#2	#3	#4
Cu-tube				
Diameter (mm)	6.2	4.8	4.8	4.8
Wall Thickness (mm)	0.8	0.8	0.8	0.8
Cyl. Container				
Diameter (cm)	12.7	15.2	12.5	12.5
Height (cm)	38.1	17.1	16.0	16.0
Explosive Load (g)	2,270	1,590	1,021	1,077
Density of Nitro- guanidine (g /cm ³)	0.47	0.51	0.52	0.55
Diameter of Reaction Zone (mm)	1.3*	0.9 ⁺	0.7 ⁺	1.1 0.8 ^a
Transition Tem- perature (K)	8.24	8.36	8.5	8.5
Remarks	No evacuation		He-purged	

*well defined

⁺diffuse^adiameter of hole

A more extensive study of sample #2, by X-ray microprobe analysis [19], yielded no significant additional information about the nature of the phases present. A scanning electron photomicrograph showing the extent of the reaction zone is given in Figure 15. Extensive cracks are formed in the center during the rapid cooling process due to differences in the expansion coefficients. With higher magnification (1000 X), an intermetallic compound with dendritic growth-possibly the compound Nb_5Ge_3 [19]-is observed in this sample, as is shown in Figure 16a. Figure 16 also contains images of the characteristic radiation of both the niobium and the germanium in the reaction area, as well as in the outer unreacted but highly compacted zone. The difference in the distribution and a gradual change in concentration of Nb and Ge in the reaction area is clearly visible, giving evidence of the compound formation.

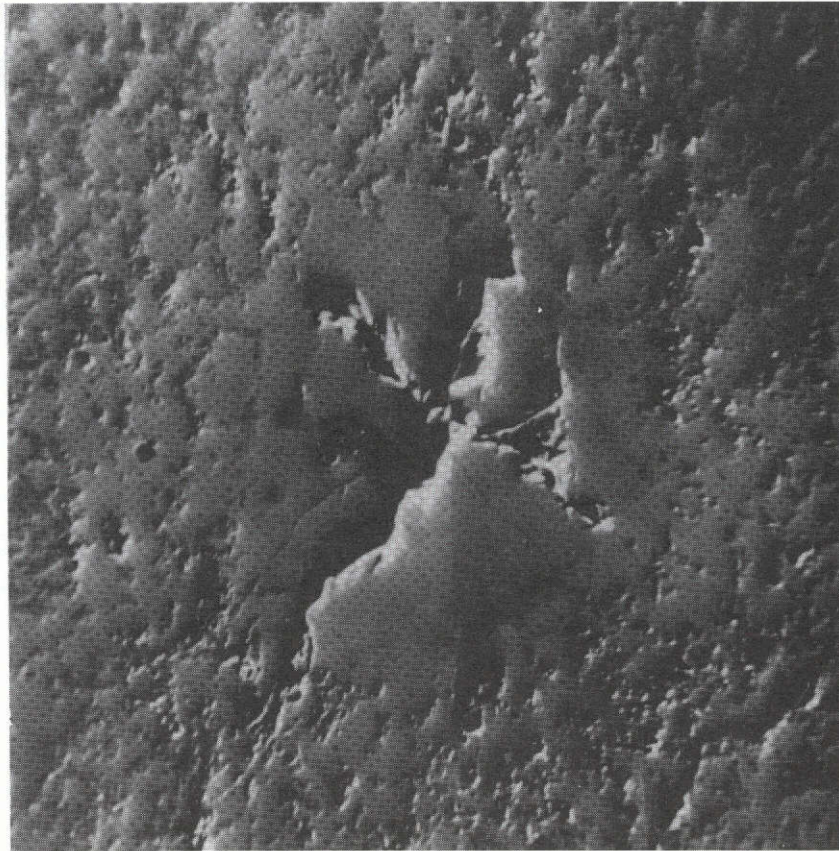
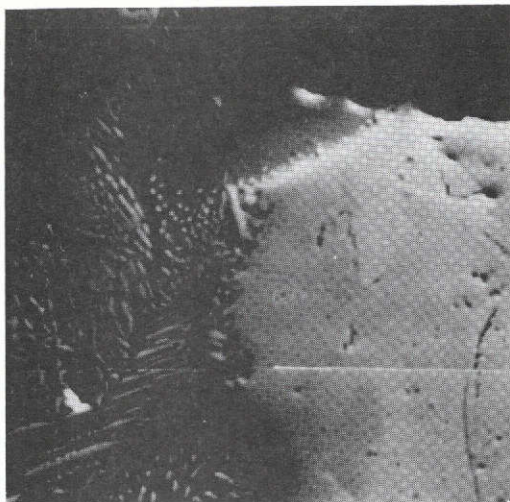
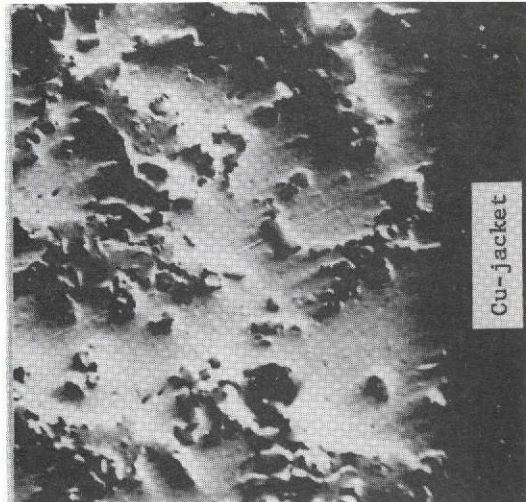


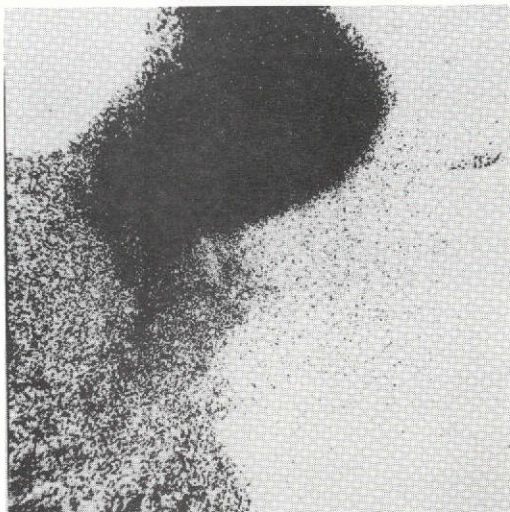
Figure 15: Scanning electron photomicrograph of a compacted 3Nb:1Ge powder mixture, (Specimen #2). Magnification 100 X.



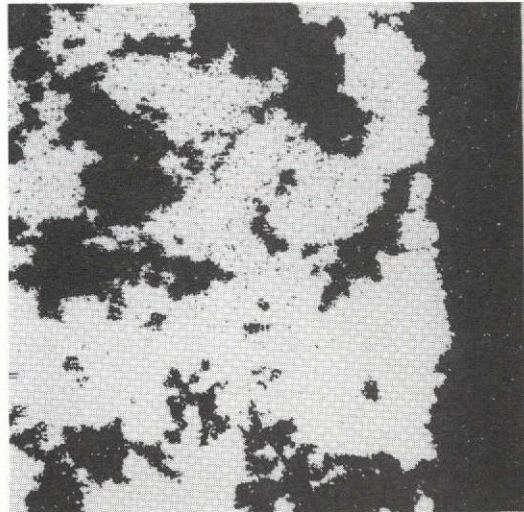
a. SEI-Image 1000X



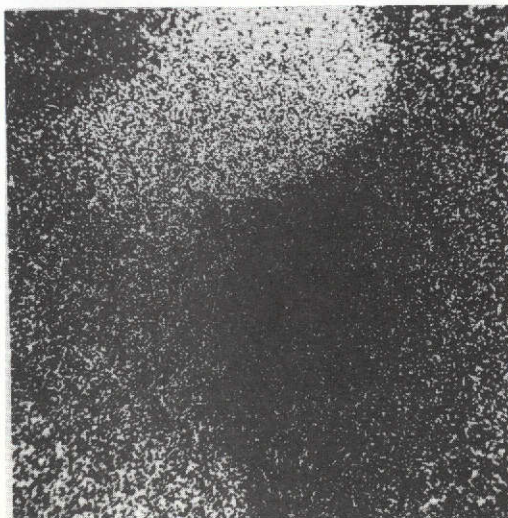
d. SEI-Image 330X



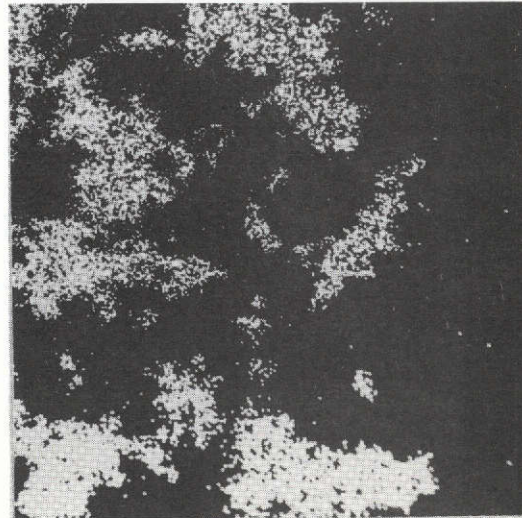
b. NbL $_{\alpha 1}$ -Image 1000X



e. NbL $_{\alpha 1}$ -Image 330X



c. GeK $_{\alpha 1}$ -Image 1000X



f. GeK $_{\alpha 1}$ -Image 330X

Fig.16: X-ray microprobe analyses of specimen #2; 3Nb:1Ge. Left column: reaction zone, right column: unreacted area.

IV. SHOCK WAVE PROPAGATION

In a schematic fashion, the propagation of a shock wave or pressure pulse in different materials will be considered and the basic difference in the absorption of the wave will be illustrated. As can be seen from Figure 2, a cylindrical symmetry has been chosen for the set-up. The components of motion of the generated pressure pulse are towards the center as well as along the cylindrical symmetry axis. For the compaction process itself, the movement of the shock wave along the sample is not important and, therefore, we will consider the collision of a circular shock wave in two dimensions only.

The peak pressure (p) generated by the decomposition of the explosive powder is generally proportional to the square of its detonation velocity [20]. The following relationship holds for the generated pressure:

$$p = 2.5 \rho v_d^2 \quad (1)$$

where ρ (g/cm^3) is the density of the explosive and v_d (km/sec) is its characteristic detonation velocity. Using the dimensions as indicated for ρ and v_d the peak pressure is obtained in kilobar ($1 \text{ kbar} = 1000 \text{ atm.}$). Table 5 lists for a selected number of commonly available explosives the calculated peak pressures. It may be seen that the useful pressure range for nitroguanidine because of its variable density extends over a range of three. The relationship between v_d and ρ has been measured for nitroguanidine [21] and some results are given in Figure 17. It can be seen that the detonation velocities achieved are not too high; however, the shock pressure will be increased in the experiment because of the converging nature of the pulse. It is important to note that the amount of explosive

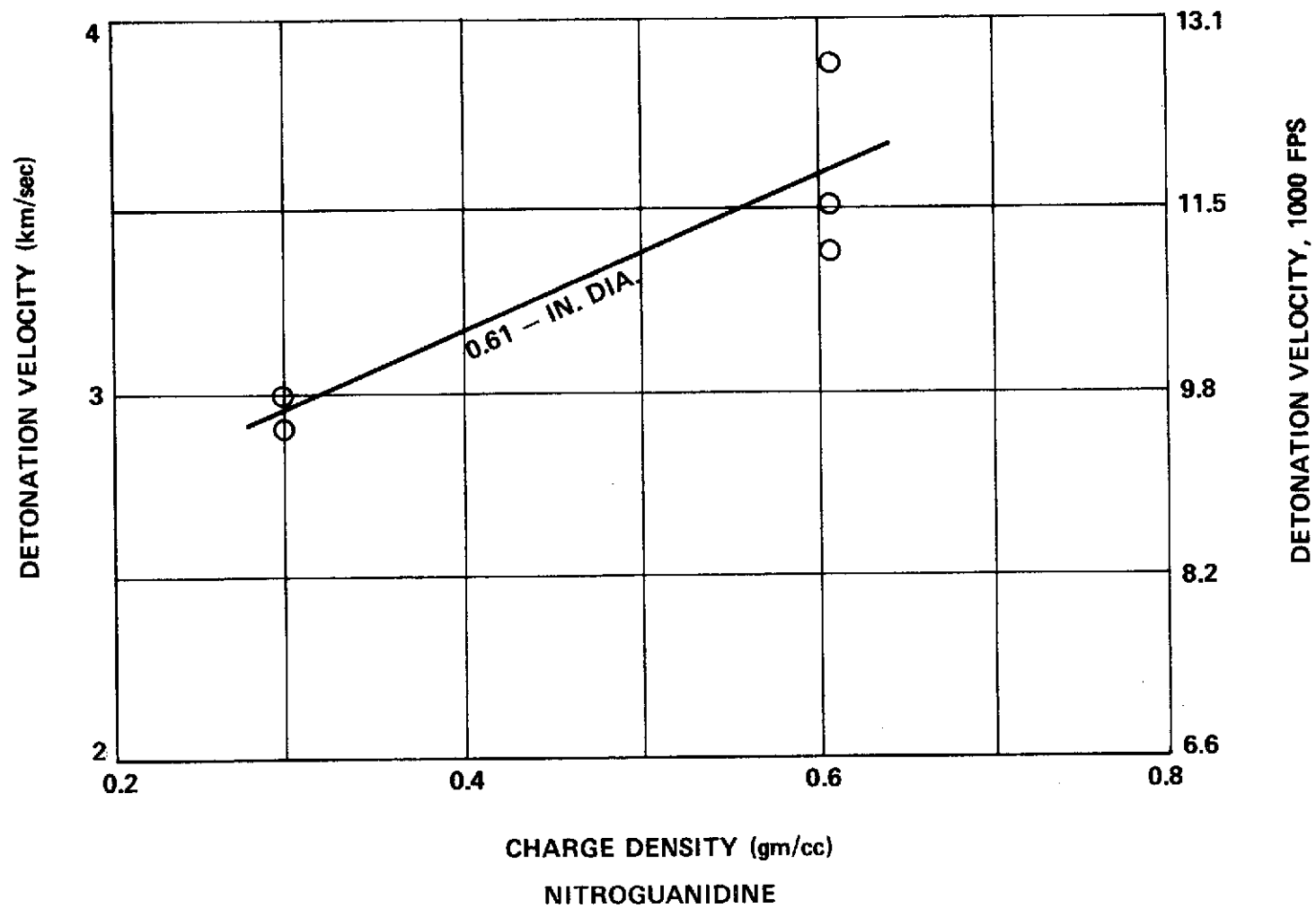


Figure 17. Detonation velocity and charge density for nitroguanidine.

used has little effect on the peak pressure itself but is mainly responsible for the duration of the pressure pulse, which is in the order of micro-seconds [22].

Table 5 Peak Pressures for Commonly Used Explosives (Partially from [20])

Explosive	Density (g/cm ³)	Detonation Velocity (km/sec)	Pressure (kbar)
Carbonit	1.0	1.72	7.4
NG	0.3	2.95	6.5
NG	0.6	3.6	19.4
Ammonit	0.95	4.0	38
TNT	1.64	6.9	195

Once the shock wave enters the copper housing of the sample, it propagates as a compaction wave through the material. Two competing processes are then taking place:

- i The energy of the converging shock wave is absorbed by plastic deformation of the powder, grain fracturing, phase transformations, and oblique reflections.
- ii The energy density of shock wave is increased because of the converging nature of the pressure pulse.

Depending on which one of the two processes dominates, the net shock pressure towards the center can be either greater or less than the calculated pack pressure.

The described processes may be approached analytically [23] by using an absorption coefficient (A), whereby the pressure decreases exponentially towards the center of the sample, and a simultaneous increase of pressure with

$1/x$, taking into account the converging nature of the wave. The following relation can then be used:

$$P(x) = p_0 \frac{R}{x} e^{-A(x-R)} \quad (2)$$

where p_0 is the pressure on the outside of the copper tube, $2R$ is the outside diameter of the tube, and x is the distance of a specific location from the center of the sample.* The absorption coefficient A is dependent on the kind of material compacted. The magnitude of A would be controlled by quantities like the plastic deformability, fracturization of grains, or reflective losses on interfaces.

Starting with the presumption, that an optimum pressure is required for the compaction of a certain material, the importance of the absorption coefficient becomes eminent. Assuming a strong absorption, it may occur that only an outer shell of the powder is compacted; whereas the center area is uncompacted. This effect to a certain extent is observed in sample 56 (V_3Si). The other extreme would be that the absorption is so small that a good compaction may only be obtained in the center of the sample. Since an increase in shock pressure coincides with an increase of the wave velocity, the collision of the particles in the center (focus) may be so severe that the formation of a hole occurs. This has been found in the case of Nb_3Sn for packing densities of the NG greater than 0.6 g/cm^3 . Compared with pure niobium powder the compound powders exhibit a larger absorption coefficient because of the energy needed for fracturing of the grains. Since the Al5 powders have extremely low compressibility, a fracturing of the material during shock wave passage is the necessary consequence and no pressure or strain will be frozen in.

* This equation contains the experimentally not verified situation that the pressure in the center of the sample ($x=0$) is infinite.

V. CONCLUSIONS AND RECOMMENDATIONS

We have shown that brittle powders of high T_c Al5 superconductors can be compacted by shock waves. The shock wave passage through the powder leads to a severe fracturing of the individual grains, and a size of particles as small as $1\text{ }\mu\text{m}$ in diameter has been observed. This fracturing is found responsible for a lowering of the transition temperature of the superconductor. This investigation has not yet established if the T_c can again be increased by a subsequent annealing of the materials. The decrease in the transition temperature has been observed for all investigated compounds regardless of their superconducting pressure coefficient. Since the transition temperature was not raised after shock wave compaction, it can be concluded in the case of V_3Si that no pressure was frozen in. Otherwise the T_c should have been increased, because of the positive pressure coefficient for V_3Si .

It is, therefore, anticipated that other Al5 compounds like Nb_3Au or Nb_3Os will exhibit also a transition temperature decrease after shock wave compaction.

The formation of compounds from their elemental constituents by the explosive compaction of powders could be established for the binary system Nb-Ge. However, the formation of the intermetallic compound Nb_3Ge was not observed. The compaction of other binary powder mixtures forming compounds with the Al5 structure needs additional investigations.

REFERENCES

1. Gavalier, J. R., M. A. Janocko, and C. K. Jones: J. of Appl. Physics 45, 3009 (1974).
2. VanReuth, E. C. and R. M. Waterstrat: Acta Cryst. B24, 126 (1968).
3. Matthias, B. T., T. H. Geballe, R. H. Willens, E. Corenzwit, and G. W. Hull: Phys. Rev. 139, A1501 (1965).
4. McCarthy, S. L.: J. of Low Temp. Physics 4, 669 (1971).
5. Arrhenius, G., E. Corenzwit, R. Fitzgerald, G. W. Hull, H. L. Luo, B. T. Matthias, and W. H. Zachariasen: Proc. Natl. Acad. Sci. USA 61, 621 (1968).
6. Hein, R. A., J. E. Cox, R. D. Blaugher, R. M. Watersrat, and E. C. VanReuth: Proc. of the Int. Conf. on the Science of Superconductivity. F. Chilton, Ed. North Holland Publ. Co. 1971, p. 523.
7. Deaton, B. C. and D. E. Gordon: Thirteenth Int. Conf. on Low Temp. Physics, Boulder, Colorado-Aug. 1972.
8. Otto, G., O. Y. Reece, and U. Roy: Appl. Phys. Letters, 18, 418 (1971).
9. Otto, G., U. Roy, and O. Y. Reece: J. Less-Common Metals 32, 355 (1973).
10. Smith, T. F.: J. of Low Temp. Physics 6, 171 (1972)
11. Neubauer, H. : Z. Physik 226, 211 (1969).
12. Blaugher, R. D., R. E. Hein, J. E. Cox, and R. M. Waterstrat: J. Low Temp. Phys. 1, 539 (1969).
13. Koch, C. C. and J. O. Scarbrough: Phys. Rev. B3, 742 (1971).
14. Otto, G. : Z. Physik 215, 323 (1968)
15. Roy, U., G. H. Otto, and O. Y. Reece: U. S. Patent #3,752,665; August 14, 1973.
16. Hardy, G. and J. K. Hulm: Phys. Rev. 89, 884 (1953).
Otto, G. : Z. Physik 218, 52 (1969).
17. Gavalier, J. R.: Appl. Phys. Letters 23, 480 (1973).
18. Testardi, L. R., J. H. Wernick, and W. A. Royer: Solid State Comm. 15, 1 (1974).
19. G. L. Horn; DODUCO K. G., Pforzheim/West Germany, Private Communication.

20. Pruemmer, R.: Ber. Dt. Keram. Ges. 50, 75 (1973).
21. Reece, O. Y., Marshall Space Flight Center, Private Communication.
22. Kinney, G. F.: "Explosive Shocks in Air", The MacMillan Co., New York, N. Y. 1962 p. 82.
23. Pruemmer, R., Fraunhofer-Gesellschaft, Amstetten/West Germany. Private Communication.